A multi-scale patch approximation for Poisson problems with a small inhomogeneous inclusion

Saber Amdouni, Mohamed Khaled Gdoura, Arnaud Heibig, Thomas Homolle, Nidhal Mannai, Adrien Petrov, Yves Renard

A multi-scale patch approximation for Poisson problems with a small inhomogeneous inclusion

Saber Amdouni* Mohamed Khaled Gdoura* † Arnaud Heibig‡ Thomas Homolle§
Nidhal Mannai* Adrien Petrov‡ Yves Renard‡

December 16, 2023

Abstract

The paper deals with the multi-scale approximation of the influence of a small inhomogeneity of arbitrary shape in an elastic medium. A new multi-scale patch method is introduced, whose caracteristic is to deal with a large scale problem without inclusion, a small-scale problem on a patch surrounding the inclusion defining a corrector and an iterative procedure between these two problems. Theoretical results of convergence of the iterations, a posteriori error estimate and comparison of the corrector with the asymptotic expansion are provided. The finite element approximation is also addressed together with some numerical tests.

Key words. Patch method, Asymptotic expansion, finite element method, multi-scale analysis, transmission problem

1 Introduction

An important engineering and mathematical literature is devoted to inclusions embedded in elastic media as for instance in automotive industry to design tires having specific structure stiffnesses. A good understanding of these inclusions influence is crucial to preserve the quality required by the traffic safety and driver comfort as well as to reduce maintenance costs. We are particularly interested in this work to some small elastic inhomogeneous inclusions in a two-dimensional elastic body. Without adapted treatment, the numerical approximation of this problem requires a mesh refinement near the inclusions which is rather costly from numerical viewpoint, especially when the inclusion is small compared to the domain

*Laboratory For Mathematical And Numerical Modeling In Engineering Science, LAMSIN, LR99ES20, University of Tunis El Manar, National Engineering School of Tunis, Tunis, Tunisia (saber.amdouni@enit.utm.tn, nidhal.mannai@enit.utm.tn)

†University of Carthage, National Institute of Applied Science and Technology, Centre Urbain Nord BP 676-1080 Tunis Cedex, Tunisia (mk.gdoura@insat.ucar.tn)

‡Univ Lyon, INSA Lyon, UJM, UCBL, ECL, CNRS UMR 5208, ICJ, F-69621, France (arnaud.heibig@insa-lyon.fr, apetrov@math.univ-lyon1.fr, yves.renard@insa-lyon.fr)

§Numerical Modeling and Simulation (FEA) Department of Simulation and Data-Science, Manufacture Française des Pneumatiques Michelin Center of Technologies, Ladoux, Clermont-Ferrand, France (thomas.homolle@michelin.com)

of interest. The homogenization techniques can be used in the particular case where the inclusions are arranged within a periodic or nearly periodic network. The reader is referred for instance to [1, 28] for further details. However, these techniques are not convenient when one needs to evaluate the influence of isolated inclusions. These inclusions are often omitted in many applications at least for the smallest ones because of the induced computational cost. The asymptotic analysis could be used to determine isolated inclusions influence, see for instance [6, 7, 11, 12, 20, 22, 34, 36] and the references therein. The numerical method we propose is inspired by the asymptotic analysis presented in [5].

This paper focuses on an approximation of the influence of a small inhomogeneity in an elastic medium by the construction of a patch type method. This method allows to compute successive approximations of the deformation, starting from the deformation without the inclusion. Unlike the analytical approaches derived from Eshelby's seminal work [17] and various extensions analyzed later on in [18, 31, 24, 25, 4, 35, 27], the considered inclusion is of arbitrary geometry and elastic property. The proposed method is close to the Schwarz type domain decomposition method with total overlap (see [14] for instance) as well as to the patch methods described in [21, 30, 32], except that here, the micro and large scale problems do not take into account the same physics. It is also close to the structural zoom methods [13, 10] with the main difference of starting from the solution without inclusion and iterating on correctors to this solution. This last characteristic has the advantage of being less intrusive for an existing finite element code (the large scale computation is performed on the whole geometry without taking into account the inclusion) and it allows the link with the asymptotic analysis developed in [5] and unable us to guarantee some approximation orders.

The paper is organized as follows. In this work, we are interested in a transmission problem between a body and an inhomogeneous inclusion both being elastic. More precisely, a geometrical setting is presented and the solvability is recalled in Section 2. Our *patch method* is introduced in Section 3. This method consists to incorporate an intermediate polygonal domain, so-called influence domain or Patch domain, which contains the inclusion. Hence a corrector is evaluated on the patch domain by using a mesh refinement and added to the solution without inclusion evaluated on the whole domain by using a coarse mesh. This procedure can be iterated to improve the approximation accuracy. Some convergence results of the iterations to the solution of the transmission problem are given. Then, Section 4 makes the link between our patch method and the asymptotic analysis in [5]. In the particular case of Dirichlet condition on the boundary of the domain, it allows us to state an order of convergence with respect to the inclusion and patch sizes for the corrector on the first iteration. Finally, the numerical patch method is introduced in Section 5 with a two-scale finite element approximation and some numerical tests on a simple geometry and a circular inclusion are presented in Section 6 that are compared to the theoretical results of sections 3 and 4.

2 Mathematical formulation of the transmission problem

Let Ω be a bounded Lipschitz domain in $\mathbb{R}^2$ with a Lipschitz-continuous external boundary $\Gamma = \partial\Omega$. Let Ω_f^1 a bounded connected domain of characteristic dimension 2 representing the geometry of the inclusion, and $\Omega_f = \varepsilon\Omega_f^1$ the domain of characteristic dimension 2ε representing the inclusion, satisfying $\Omega_f \subset \Omega$. Let $\Gamma^\varepsilon = \partial\Omega_f$ be the curve separating the two domains and $\Omega_m \overset{\text{def}}{=} \Omega\backslash\bar{\Omega}_f$ the rest of the domain. The inclusion is assumed to be small enough compared to the characteristic size R of the domain Ω. We assume also that the boundary Γ is split into two disjoint sets Γ_{D} and Γ_{N} where Dirichlet and Neumann

boundary conditions are considered, respectively. Finally, we denote by Λ a *patch domain* supposed to be included in Ω and containing Ω_f (for ε of interest) and by $\partial\Lambda$ its boundary (see Figure 1).

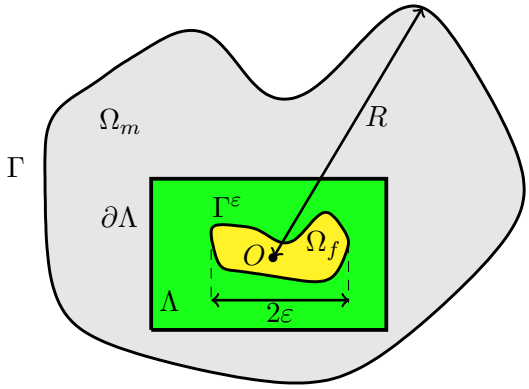

Figure 1: A small inclusion in an elastic medium

We focus in this work on a two-dimensional multi-scale problem with discontinuous coefficient α across Γ^ε. Let $u : \Omega \to \mathbb{R}^2$, be the displacement of the body Ω and h be the prescribed Neumann boundary condition on Γ_{N}. The mathematical problem is formulated as follows

$$-\alpha_f \Delta u_f = f \quad \text{in} \quad \Omega_f, \tag{2.1a}$$
$$-\alpha_m \Delta u_m = f \quad \text{in} \quad \Omega_m, \tag{2.1b}$$
$$u_f = u_m \quad \text{on} \quad \Gamma^\varepsilon, \tag{2.1c}$$
$$\alpha_f \frac{\partial u_f}{\partial n} = \alpha_m \frac{\partial u_m}{\partial n} \quad \text{on} \quad \Gamma^\varepsilon, \tag{2.1d}$$
$$u = 0 \quad \text{on} \quad \Gamma_{\mathrm{D}}, \tag{2.1e}$$
$$\frac{\partial u}{\partial n} = h \quad \text{on} \quad \Gamma_{\mathrm{N}}, \tag{2.1f}$$

where $\frac{\partial}{\partial n}$ denotes the normal derivative, $\alpha_f > 0$ and $\alpha_m > 0$ are the constant shear coefficients in the inclusion and in the matrix, respectively, while u_f and u_m are the restriction of u to Ω_f and Ω_m, respectively. A perfect transmission conditions of u and its normal derivative is assumed. We denote by u^0 the solution to the problem without any inclusion which reads:

$$-\alpha_m \Delta u^0 = f \quad \text{in} \quad \Omega, \tag{2.2a}$$
$$u^0 = 0 \quad \text{on} \quad \Gamma_{\mathrm{D}}, \tag{2.2b}$$
$$\frac{\partial u^0}{\partial n} = h \quad \text{on} \quad \Gamma_{\mathrm{N}}. \tag{2.2c}$$

We describe the weak formulation associated to problems (2.1) and (2.2). To this aim, we introduce the following vector space:

$$\mathcal{V}_0 \overset{\text{def}}{=} \{v \in \mathrm{H}^1(\Omega) : \ v_{|\Gamma_{\mathrm{D}}} = 0\}. \tag{2.3}$$

We state the problem (2.1) in a variational form as

$$\begin{cases} \text{find } u \in \mathcal{V}_0 \text{ such that for all } v \in \mathcal{V}_0, \\ \displaystyle\int_{\Omega_m} \alpha_m \nabla u \cdot \nabla v \,\mathrm{d}x + \int_{\Omega_f} \alpha_f \nabla u \cdot \nabla v \,\mathrm{d}x = \int_{\Omega} f v \,\mathrm{d}x + \int_{\Gamma_{\mathrm{N}}} h v \,\mathrm{d}S, \end{cases} \tag{2.4}$$

while the variational form associated to problem (2.2) is given by

$$\begin{cases} \text{find } u^0 \in \mathcal{V}_0 \text{ such that for all } v \in \mathcal{V}_0, \\ \displaystyle\int_{\Omega} \alpha_m \nabla u^0 \cdot \nabla v \,\mathrm{d}x = \int_{\Omega} f v \,\mathrm{d}x + \int_{\Gamma_{\mathrm{N}}} h v \,\mathrm{d}S. \end{cases} \tag{2.5}$$

We assume that $h \in \mathrm{L}^2(\Gamma_{\mathrm{N}})$ and $f \in \mathrm{L}^2(\Omega)$. The existence and uniqueness results to problems (2.4) and (2.5) follow from Lax-Milgram's theorem. We denote in the sequel by $C > 0$ a generic constant depending only on the data and $C_{\alpha_f,\alpha_m} \overset{\text{def}}{=} \sqrt{\frac{|\alpha_m - \alpha_f|}{\alpha_f}}$.

3 The patch method

We introduce in this section an iterative procedure allowing to approximate the solution u starting from u^0, the solution which does not take into account the inclusion. To this aim, we define a corrector on the patch Λ and an iterative method allowing to progressively take into account the influence of the inclusion in the large-scale solution. We define w^i and u^i, $i \in \mathbb{N} \cup \{-1\}$, intended to capture the inclusion influence with precision and to report this influence in the whole domain, respectively. The main difference between the algorithm introduced below and the *domain decomposition* [14] or the *zoom method* [10] comes from the multi-physical aspect added to multi-scale nature of the problem.

It is convenient to introduce also the following notations; let $\langle u, v \rangle_{\alpha,\Omega} \overset{\text{def}}{=} \displaystyle\int_{\Omega} \alpha \nabla u \cdot \nabla v \,\mathrm{d}x$ be the scalar product and $\|u\|^2_{\alpha,\Omega} \overset{\text{def}}{=} \displaystyle\int_{\Omega} \alpha |\nabla u|^2 \,\mathrm{d}x$ the associated norm for all $(u, v) \in \mathrm{H}^1(\Omega) \times \mathrm{H}^1(\Omega)$, where

$$\alpha \overset{\text{def}}{=} \begin{cases} \alpha_f & \text{in} \quad \Omega_f, \\ \alpha_m & \text{in} \quad \Omega_m, \end{cases}$$

and let

$$\mathcal{W}_0 \overset{\text{def}}{=} \{v \in \mathrm{H}^1(\Omega) : v_{|\Omega \setminus \Lambda} = 0\},$$

be the Hilbert space whose associated scalar product is $\langle \cdot, \cdot \rangle_{\alpha,\Lambda}$. We denote by $\mathrm{Proj}_{\mathcal{W}_0} : \mathrm{H}^1(\Lambda) \to \mathrm{H}^1_0(\Lambda)$ the orthogonal projection onto $\mathcal{W}_0$ relatively to this scalar product. Notice that $\mathcal{W}_0$ is isomorphic to $\mathrm{H}^1_0(\Lambda)$.

3.1 The multi-scale patch method iteration

This section is dedicated to develop a multi-scale patch iterative strategy in order to approximate u the solution of the interface problem (2.1). Let $w^{-1} = u^{-1} = 0$ be the first terms of the iterative procedure.

For any $w^{n-1} \in \mathcal{W}_0$ and $u^{n-1} \in \mathcal{V}_0$ given, $n \geq 0$, u^n is the solution to the following macroscopic problem on the whole domain Ω:

$$\begin{cases} \text{find } u^n \in \mathcal{V}_0 \text{ such that for all } v \in \mathcal{V}_0, \\ \displaystyle\int_\Omega \alpha_m \nabla u^n \cdot \nabla v \,\mathrm{d}x = \int_\Omega f v \,\mathrm{d}x + \int_{\Gamma_N} h v \,\mathrm{d}S \\ \displaystyle -\int_{\Omega_f} (\alpha_f - \alpha_m) \nabla u^{n-1} \cdot \nabla v \,\mathrm{d}x - \int_\Lambda \alpha \nabla w^{n-1} \cdot \nabla v \,\mathrm{d}x, \end{cases} \tag{3.1}$$

and w^n is the solution to the microscopic problem on the patch Λ:

$$\begin{cases} \text{find } w^n \in \mathcal{W}_0 \text{ such that for all } v \in \mathcal{W}_0, \\ \displaystyle\int_\Lambda \alpha \nabla w^n \cdot \nabla v \,\mathrm{d}x = \int_\Lambda f v \,\mathrm{d}x - \int_\Lambda \alpha \nabla u^n \cdot \nabla v \,\mathrm{d}x. \end{cases} \tag{3.2}$$

Note that the method is constructed such that u^0 is the solution to problem without inclusion (2.5).

3.2 Convergence of the iterations

We establish below that $u^n + w^n$ converges toward the solution u to problem (2.4). To this aim, let us introduce

$$a^n \overset{\text{def}}{=} u - (u^n + w^{n-1}) \quad \text{and} \quad b^n \overset{\text{def}}{=} u - (u^n + w^n) \tag{3.3}$$

for all $n \in \mathbb{N}$. Observe that a^n and b^n belong to $\mathrm{H}^1(\Omega)$.

Firstly we prove that $\|b^n\|_{\alpha,\Omega} \leq \|a^n\|_{\alpha,\Omega}$ and secondly we discuss the conditions under which $\|a^n\|_{\alpha,\Omega} \leq K \left\|b^{n-1}\right\|_{\alpha,\Omega}$ with $K < 1$ in order to ensure that $\|b^n\|_{\alpha,\Omega}$ decreases to zero.

Lemma 3.1. *Assume that u, u^n and w^n be the solutions to problems* (2.4)*,* (3.1) *and* (3.2)*, respectively and* (3.3) *holds. Then, we have*

$$\|b^n\|_{\alpha,\Omega} \leq \|a^n\|_{\alpha,\Omega} \tag{3.4}$$

for all $n \in \mathbb{N}$.

Proof. Since u is the solution to problem (2.4), it comes that

$$\int_\Lambda \alpha \nabla u \cdot \nabla v \,\mathrm{d}x = \int_\Lambda f v \,\mathrm{d}x \tag{3.5}$$

for all $v \in \mathcal{W}_0$. By subtracting (3.5) from (3.2), we get

$$\int_\Lambda \alpha \nabla w^n \cdot \nabla v \,\mathrm{d}x = \int_\Lambda \alpha \nabla (u - u^n) \cdot \nabla v \,\mathrm{d}x$$

for all $v \in \mathcal{W}_0$. Clearly, we may infer that $w^n = \mathrm{Proj}_{\mathcal{W}_0}(u - u^n)$ and it follows that

$$\|u - (u^n + w^n)\|_{\alpha,\Lambda} \leq \left\|u - (u^n + w^{n-1})\right\|_{\alpha,\Lambda}. \tag{3.6}$$

On the other hand, we have

$$\|u - (u^n + w^n)\|^2_{\alpha,\Omega} = \|u - u^n\|^2_{\alpha,\Omega\setminus\Lambda} + \|u - (u^n + w^n)\|^2_{\alpha,\Lambda}. \tag{3.7}$$

Carrying (3.6) into (3.7), the desired result follows. □

Note that subtracting (3.5) from (3.2), we obtain the following identity:

$$\int_\Lambda \alpha \nabla b^n \cdot \nabla v \, \mathrm{d}x = 0 \tag{3.8}$$

with $v \in \mathcal{W}_0$. The next step consists to establish that there exists $K(\varepsilon, \alpha_f, \alpha_l) \in]0,1[$, depending on ε, α_f and α_m such that

$$\|a^n\|_{\alpha,\Omega} \leq K(\varepsilon, \alpha_f, \alpha_l) \left\|b^{n-1}\right\|_{\alpha,\Omega}. \tag{3.9}$$

We deduce from (2.4) and (3.1) that

$$\begin{aligned}\int_\Omega \alpha_m \nabla u^n \cdot \nabla v \, \mathrm{d}x &= \int_\Omega \alpha_m \nabla u \cdot \nabla v \, \mathrm{d}x - \int_\Lambda \alpha_m \nabla w^{n-1} \cdot \nabla v \, \mathrm{d}x \\ &+ \int_{\Omega_f} (\alpha_f - \alpha_m) \nabla (u - (u^{n-1} + w^{n-1})) \cdot \nabla v \, \mathrm{d}x\end{aligned}$$

for all $v \in \mathcal{V}^0$, which according to notations (3.3) implies that

$$\int_\Omega \alpha_m \nabla a^n \cdot \nabla v \, \mathrm{d}x = -\int_{\Omega_f} (\alpha_f - \alpha_m) \nabla b^{n-1} \cdot \nabla v \, \mathrm{d}x \tag{3.10}$$

for all $v \in \mathcal{V}^0$. Choosing $v = a^n$ in (3.10), we get

$$\int_\Omega \alpha \left|\nabla a^n\right|^2 \mathrm{d}x = \int_{\Omega_f} (\alpha_f - \alpha_m) \left|\nabla a^n\right|^2 \mathrm{d}x - \int_{\Omega_f} (\alpha_f - \alpha_m) \nabla b^{n-1} \cdot \nabla a^n \, \mathrm{d}x.$$

According to Cauchy-Schwarz's inequality, we find

$$\|a^n\|^2_{\alpha_m,\Omega_m} + \frac{\alpha_m}{\alpha_f} \|a^n\|^2_{\alpha_f,\Omega_f} = -\frac{\alpha_f - \alpha_m}{\alpha_f} \int_{\Omega_f} \alpha_f \nabla b^{n-1} \cdot \nabla a^n \, \mathrm{d}x \leq C^2_{\alpha_f,\alpha_m} \|a^n\|_{\alpha_f,\Omega_f} \left\|b^{n-1}\right\|_{\alpha_f,\Omega_f}. \tag{3.11}$$

On the one hand, using Young's inequality, we infer from (3.11) that for all $\gamma > 0$ we have

$$\|a^n\|^2_{\alpha_m,\Omega_m} + \frac{\alpha_m}{\alpha_f} \|a^n\|^2_{\alpha_f,\Omega_f} \leq C^2_{\alpha_f,\alpha_m} \Big(\gamma \|a^n\|^2_{\alpha_f,\Omega_f} + \frac{1}{4\gamma} \left\|b^{n-1}\right\|^2_{\alpha_f,\Omega_f} \Big).$$

Taking $\frac{\alpha_m}{\alpha_f} \geq 1$ and $\gamma = 1$, we obtain

$$\|a^n\|^2_{\alpha,\Omega} \leq \frac{1}{4} \Big(\frac{\alpha_m}{\alpha_f} - 1 \Big) \left\|b^{n-1}\right\|^2_{\alpha_f,\Omega_f}. \tag{3.12}$$

On the other hand, (3.11) implies that

$$\min\Big(1, \frac{\alpha_m}{\alpha_f}\Big) \|a^n\|_{\alpha,\Omega} \leq C^2_{\alpha_f,\alpha_m} \left\|b^{n-1}\right\|_{\alpha_f,\Omega_f}. \tag{3.13}$$

Hence we may deduce from (3.12) and (3.13) that for $\frac{1}{2}\alpha_f < \alpha_m < 5\alpha_f$, $\|b^n\|_{\alpha,\Omega} \leq C(\alpha_m,\alpha_f)\,\|b^n\|_{\alpha,\Omega}$ with $C(\alpha_m,\alpha_f) < 1$. Consequently, b^n converges to 0 in $\mathrm{H}^1(\Omega)$. However, this result can be improved as we will see later on. To this aim, we define the two following auxiliary problems:

$$\begin{cases} \text{find } \zeta \in \mathrm{H}^1(\Lambda) \text{ with } \zeta = q \text{ on } \partial\Lambda \text{ such that for all } z \in \mathcal{W}_0, \\ \langle \zeta, z\rangle_{\alpha_m,\Lambda} \stackrel{\text{def}}{=} \displaystyle\int_\Lambda \alpha_m \nabla\zeta\cdot\nabla z\,\mathrm{d}x = 0, \end{cases} \tag{3.14}$$

and

$$\begin{cases} \text{find } \eta \in \mathrm{H}^1(\Lambda) \text{ with } \eta = q \text{ on } \partial\Lambda \text{ such that for all } z \in \mathcal{W}_0, \\ \langle \eta, z\rangle_{\alpha,\Lambda} \stackrel{\text{def}}{=} \displaystyle\int_\Lambda \alpha \nabla\eta\cdot\nabla z\,\mathrm{d}x = 0. \end{cases} \tag{3.15}$$

The existence and uniqueness results to problem (3.14) and (3.15) follow from Lax-Milgram's theorem, the verification is let to the reader. Under appropriate regularity assumptions on boundary conditions, we establish below that $\|\zeta\|_{\alpha_f,\Omega_f}$ and $\|\eta\|_{\alpha_f,\Omega_f}$ being limited to $\mathcal{O}(\varepsilon)$. We will use the following notations in the sequel: $\mathcal{X} \stackrel{\text{def}}{=} \mathrm{H}^{1/2}(\partial\Lambda)$ and $\mathcal{X}' \stackrel{\text{def}}{=} \mathrm{H}^{-1/2}(\partial\Lambda)$.

Lemma 3.2. *Assume that $q \in \mathcal{X}$ and ζ be the solution to problem* (3.14)*. Then, there exists a constant $C > 0$, independent of ε, such that*

$$\|\zeta\|_{\alpha_f,\Omega_f} \leq C\varepsilon\,\|q\|_{\mathcal{X}}\,. \tag{3.16}$$

Proof. Let $\mathcal{C}_\varrho$ be a disk of radius $\varrho > 0$ such that $\Omega_f \subset \mathcal{C}_{\varrho/2} \subset \mathcal{C}_\varrho \subset \Lambda$ and $0 < \varepsilon < \varepsilon_0$ small enough. For any $(x,y) \in \mathcal{C}_{\varrho/2}$, let $z \stackrel{\text{def}}{=} x + iy$, and we can express the Poisson kernel as follows:

$$\zeta(x,y) = \Re f(z) \quad \text{with} \quad f(z) \stackrel{\text{def}}{=} \frac{1}{2\pi}\int_{-\pi}^{\pi} \frac{\varrho\mathrm{e}^{i\theta}+z}{\varrho\mathrm{e}^{i\theta}-z}\,\zeta\big(\varrho\cos(\theta),\varrho\sin(\theta)\big)\,\mathrm{d}\theta.$$

For further details on the Poisson kernel, the reader is referred to [33]. Since $|z| \leq \varrho/2$, we have

$$\big|f'(z)\big| \leq \frac{1}{\pi}\int_{-\pi}^{\pi}\Big|\frac{\varrho\mathrm{e}^{i\theta}}{(\varrho\mathrm{e}^{i\theta}-z)^2}\Big|\,\big|\zeta\big(\varrho\cos(\theta),\varrho\sin(\theta)\big)\big|\,\mathrm{d}\theta \leq C\,\|\zeta\|_{\mathrm{L}^2(\partial C_\varrho)}\,.$$

Therefore, we infer that $\mathbb{R}$-euclidian norm $|\nabla\zeta(x,y)|$ satisfies

$$|\nabla\zeta(x,y)| \leq C\,\|\zeta\|_{\mathrm{L}^2(\partial C_\varrho)} \tag{3.17}$$

for all $(x,y) \in \mathcal{C}_{\varrho/2}$. We integrate (3.17) over Ω_f, we obtain

$$\|\zeta\|^2_{\alpha_f,\Omega_f} \leq C\,|\Omega_f|\,\|\zeta\|^2_{\mathrm{L}^2(\partial C_\varrho)} \leq C\varepsilon^2\,\|\zeta\|^2_{\mathrm{H}^1(\Lambda)} \leq C\varepsilon^2\,\|q\|^2_{\mathcal{X}}$$

for all $0 < \varepsilon < \varepsilon_0$, which proves the lemma. □

Lemma 3.3. *Assume that $q \in \mathcal{X}$ and η be the solution to problem* (3.15)*. Then, there exists a constant $C > 0$, independent of ε, such that*

$$\|\eta\|_{\alpha_f,\Omega_f} \leq C\varepsilon\,\|\eta\|_{\alpha,\Lambda}\,.$$

Proof. Let us define $\nu \overset{\text{def}}{=} \zeta - \eta$ where ζ and η are the solution to problems (3.14) and (3.15), respectively. Hence it comes that

$$\int_\Lambda \alpha \nabla \nu \cdot \nabla z \, \mathrm{d}x = \int_{\Omega_f} (\alpha_m - \alpha_f) \nabla \zeta \cdot \nabla z \, \mathrm{d}x,$$

for all $z \in \mathcal{W}_0$. Since $\nu \in \mathcal{W}_0$, we get

$$\|\nu\|_{\alpha,\Lambda} \leq C_{\alpha_f,\alpha_m} \|\zeta\|_{\alpha_f,\Omega_f}. \tag{3.18}$$

It follows by using the triangular inequality and (3.18) that

$$\|\eta\|_{\alpha_f,\Omega_f} \leq \left(1 + C_{\alpha_f,\alpha_m}\right) \|\zeta\|_{\alpha_f,\Omega_f}.$$

Hence, Lemma 3.2 and triangular inequality lead to

$$\|\eta\|_{\alpha_f,\Omega_f} \leq C\varepsilon \|q\|_{\mathcal{X}} \leq C\varepsilon \|\eta\|_{\alpha,\Lambda},$$

which completes the proof. □

Finally, we prove below that there exists a positive constant $K < 1$ such that

$$\|b^n\|_{\alpha,\Omega} \leq K \left\|b^{n-1}\right\|_{\alpha,\Omega} \tag{3.19}$$

for any $n \in \mathbb{N}$, provided $\varepsilon > 0$ is small enough.

Proposition 3.4. *Under the assumptions of Lemma 3.3. Then, for ε small enough and any $n \in \mathbb{N}$,* (3.19) *holds true with $K \overset{\text{def}}{=} C(\alpha_f, \alpha_m)\, \varepsilon$,*

Proof. According to Lemma 3.1, we have $\|b^n\|_{\alpha,\Omega} \leq \|a^n\|_{\alpha,\Omega}$. Since $\|a^n\|_{\alpha,\Omega} \leq C \left\|b^{n-1}\right\|_{\alpha_f,\Omega_f}$ (see (3.13)), we obtain

$$\|b^n\|_{\alpha,\Omega} \leq C \left\|b^{n-1}\right\|_{\alpha_f,\Omega_f}. \tag{3.20}$$

Appealing to (3.8) and Lemma 3.3, with $\eta = b^n$, we have

$$\left\|b^{n-1}\right\|_{\alpha_f,\Omega_f} \leq C\varepsilon \left\|b^{n-1}\right\|_{\alpha,\Lambda}. \tag{3.21}$$

Finally, (3.20) and (3.21) lead to (3.19).

□

3.3 A posteriori error estimate

The following result allows to estimate the error norm $\|b^k\|_{\alpha,\Omega}$ with respect to a norm of the correctors on the boundary of the patch. This result is of practical interest to compute an estimation of the error in a numerical procedure.

Lemma 3.5. *Still considering $b^k \overset{\text{def}}{=} u - (u^k + w^k)$, for all $k \geq 1$, we have*

$$\|b^k\|_{\alpha,\Omega} \leq C \left\| \frac{\partial w^{k-1}}{\partial n} - \frac{\partial w^k}{\partial n} \right\|_{\mathcal{X}'}.$$

Proof. If g is a function defined on Ω, we denote by g_1 and g_2 the restrictions to $\Omega\backslash\bar{\Lambda}$ and $\Lambda\backslash\bar{\Omega}_f$, respectively. Let n be the unit outward normal to the boundary of Λ.

From (3.8), we have $\Delta b^k = 0$ on Λ. Hence, by using Green's formula, we get

$$\int_\Lambda \alpha\nabla b^k\cdot\nabla v\,\mathrm{d}x = \Big\langle \alpha_m\frac{\partial}{\partial n}(u_2-(u_2^k+w_2^k)), v\Big\rangle_{\mathcal{X}',\mathcal{X}} \tag{3.22}$$

for all $v\in \mathrm{H}^1(\Omega)$. Let us define $\widetilde{\mathcal{V}}_0 \overset{\text{def}}{=} \{v\in\mathcal{V}_0, v_{|\Lambda}=0\}$. Observe that b^k is a solution to the following problem:

$$\begin{cases} \displaystyle\int_{\Omega\backslash\Lambda}\alpha\nabla b^k\cdot\nabla v\,\mathrm{d}x = 0 \text{ for all } v\in\widetilde{\mathcal{V}}_0,\\ b^k = 0 \text{ on } \Gamma_{\mathrm{D}},\quad \dfrac{\partial b^k}{\partial n} = 0 \text{ on } \Gamma_{\mathrm{N}}. \end{cases} \tag{3.23}$$

It follows that $\Delta b^k_{|\Omega\backslash\Lambda}=0$ and therefore by Green's formula leads to

$$\int_{\Omega\backslash\Lambda}\alpha\nabla b^k\cdot\nabla v\,\mathrm{d}x = -\Big\langle \alpha_m\frac{\partial}{\partial n}(u_1-u_1^k-w_1^k), v\Big\rangle_{\mathcal{X}',\mathcal{X}} \tag{3.24}$$

for all $v\in\mathcal{V}_0$. Hence, by (3.22) and (3.24), we have

$$\int_\Omega \alpha\nabla b^k\cdot\nabla v\,\mathrm{d}x = \Big\langle \alpha_m\frac{\partial}{\partial n}(u_2-u_2^k-w_2^k) - \alpha_m\frac{\partial}{\partial n}(u_1-u_1^k-w_1^k), v\Big\rangle_{\mathcal{X}',\mathcal{X}} \tag{3.25}$$

for all $v\in\mathcal{V}_0$. Next, notice that $(u-u^k-w^{k-1})\in\mathrm{H}^1(\Omega)$ satisfies

$$\int_{\Omega_m}\alpha_m\nabla(u-u^k-w^{k-1})\cdot\nabla v\,\mathrm{d}x = 0$$

for all $v\in\mathrm{H}^1_0(\Omega_m)$, due to (2.4), (3.1) and $w^{k-1}=0$ on $\Omega\backslash\Lambda$. Hence we have $\Delta\big((u-u^k-w^{k-1})_{|\Omega_m}\big)=0$ and $\Delta\big((u-u^k-w^{k-1})_{|\Omega_m}\big)\in\mathrm{L}^2(\Omega_m)$. Since $\partial\Lambda\subset\Omega_m$, we get the following jump relation:

$$\frac{\partial}{\partial n}(u_2-u_2^k-w_2^{k-1}) - \frac{\partial}{\partial n}(u_1-u_1^k-w_1^{k-1}) = 0 \text{ on } \partial\Lambda. \tag{3.26}$$

According to (3.25), (3.26) and $w_1^k = w_1^{k-1} = 0$, we obtain

$$\int_\Omega \alpha\nabla b^k\cdot\nabla v\,\mathrm{d}x = -\Big\langle \alpha_m\frac{\partial}{\partial n}(w_2^{k-1}-w_2^k), v\Big\rangle_{\mathcal{X}',\mathcal{X}} \tag{3.27}$$

for all $v\in\mathcal{V}_0$. Taking $v=b^k$ in (3.27), using Cauchy-Schwarz's and trace inequalities, the desired result follows. □

4 The patch method and asymptotic analysis approaches

The aim of this section is to describe the link between the first iteration of our patch method (namely u^0 and w^0) and the asymptotic analysis given in [5, 23]. This study is restricted to the case $\Gamma_{\mathrm{D}} = \partial\Omega$ since the asymptotic analysis has only been developed in this framework. Let us recall that the first order expansion of the problem with the small inclusion can be written

$$u(x) = u^0(x) + \varepsilon W^0\Big(\frac{x}{\varepsilon}\Big) + \mathcal{O}(\varepsilon^2),$$

where W^0 is the solution to the following problem

$$\begin{cases} \text{find } W^0 \in \widetilde{\mathcal{V}}^{R^0}_{\log} \text{ such that for all } v \in \widetilde{\mathcal{V}}^{R^0}_{\log}, \\ \displaystyle\int_{\Omega_f^1} (\alpha_f - \alpha_m)\nabla u^{(0)}(0)\cdot\nabla v\,\mathrm{d}x + \int_{\Omega_f^1}\alpha_f\nabla W^0\cdot\nabla v\,\mathrm{d}x + \int_{\Omega^\infty}\alpha_m\nabla W^0\cdot\nabla v\,\mathrm{d}x = 0, \end{cases} \tag{4.1}$$

where Ω_f^1 is Ω_f for $\varepsilon = 1$, $\Omega^\infty = \mathbb{R}\setminus\Omega_f^1$, and for a fixed $R^0 > 1$, the space $\widetilde{\mathcal{V}}^{R^0}_{\log}$ is a closed subspace of

$$\mathcal{V}_{\log} \overset{\text{def}}{=} \big\{v \in \mathcal{D}'(\mathbb{R}^2) : (1+|x|^2)^{-1/2}(\log(2+|x|^2))^{-1}v \in \mathrm{L}^2(\mathbb{R}^2) \text{ and } \nabla v \in \mathrm{L}^2(\mathbb{R}^2)^2\big\},$$

defined by

$$\widetilde{\mathcal{V}}^{R^0}_{\log} \overset{\text{def}}{=} \left\{v \in \widetilde{\mathcal{V}}_{\log} : \int_{-\pi}^{\pi} v(R^0\cos(\theta), R^0\sin(\theta))\,\mathrm{d}\theta = 0\right\},$$

and endowed with the norm

$$\|v\|_{\widetilde{\mathcal{V}}^{R^0}_{\log}} \overset{\text{def}}{=} \big(\|(1+|x|^2)^{-1/2}(\log(2+|x|^2))^{-1}v\|^2_{\mathrm{L}^2(\mathbb{R}^2)} + \|\nabla v\|^2_{\mathrm{L}^2(\mathbb{R}^2)}\big)^{1/2}.$$

For the self consistence of the paper, the estimate on the rest of the first order expansion is recalled below (see for instance [23]). The rest of the section will be dedicated to demonstrate that the difference between the corrector of the patch method w^0 and $\varepsilon W^0\big(\frac{\cdot}{\varepsilon}\big)$ is in $\mathcal{O}\big(\frac{\varepsilon^2}{\mathrm{diam}(\Lambda)}\big)$. We give also the result that $\big\|\frac{\partial w^0}{\partial n}\big\|_{\mathrm{H}^{-1/2}(\partial\Lambda)}$ is in $\mathcal{O}\big(\frac{\varepsilon^2}{\mathrm{diam}(\Lambda)^{3/2}}\big)$. These results gives also some estimates on the rest $u - (u^0 + w^0)$.

Lemma 4.1. *There exists a constant $C > 0$, independent of ε, such that*

$$\Big\|u - u^0 - \varepsilon W^0\Big(\frac{\cdot}{\varepsilon}\Big)\Big\|_{\mathrm{H}^1(\Omega)} \le C\varepsilon^2. \tag{4.2}$$

Proof. The corrector W^0 satisfies

$$\begin{aligned} &\int_{\Omega_f}(\alpha_f - \alpha_m)\nabla u^{(0)}(0)\cdot\nabla v\,\mathrm{d}x + \int_{\Omega_f}\alpha_f\nabla\Big(\varepsilon W^0\Big(\frac{\cdot}{\varepsilon}\Big)\Big)\cdot\nabla v\,\mathrm{d}x \\ &+ \int_{\Omega_m}\alpha_m\nabla\Big(\varepsilon W^0\Big(\frac{\cdot}{\varepsilon}\Big)\Big)\cdot\nabla v\,\mathrm{d}x = 0 \end{aligned} \tag{4.3}$$

for all $v \in \mathrm{H}^1_0(\Omega)$. On the other hand, by subtracting (2.4) from (2.5), we obtain

$$\int_{\Omega_f}(\alpha_f - \alpha_m)\nabla u^0\cdot\nabla v\,\mathrm{d}x + \int_{\Omega_f}\alpha_f\nabla(u-u^0)\cdot\nabla v\,\mathrm{d}x + \int_{\Omega_m}\alpha_m\nabla(u-u^0)\cdot\nabla v\,\mathrm{d}x = 0. \tag{4.4}$$

Then, it comes by subtracting (4.4) from (4.3) that

$$\begin{aligned}&\int_{\Omega_f}(\alpha_f-\alpha_m)(\nabla u^{(0)}-\nabla u^{(0)}(0))\cdot\nabla v\,\mathrm{d}x+\int_{\Omega_f}\alpha_f\nabla\Big(u-u^{(0)}-\varepsilon W^0\Big(\frac{\cdot}{\varepsilon}\Big)\Big)\cdot\nabla v\,\mathrm{d}x\\&+\int_{\Omega_m}\alpha_m\nabla\Big(u-u^{(0)}-\varepsilon W^0\Big(\frac{\cdot}{\varepsilon}\Big)\Big)\cdot\nabla v\,\mathrm{d}x=0\end{aligned}\tag{4.5}$$

for all $v\in\mathrm{H}^1_0(\Omega)$.

Let $\bar{\mathcal{L}}:\mathrm{H}^{1/2}(\Gamma)\to\mathrm{H}^1(\Omega)$ be a continuous lifting operator (see for instance [29]). We define $z^\varepsilon\overset{\text{def}}{=}\bar{\mathcal{L}}\big(-\varepsilon W^0\big(\frac{\cdot}{\varepsilon}\big)\big)$ and $\xi^\varepsilon\overset{\text{def}}{=}u-u^0-\varepsilon W^0\big(\frac{\cdot}{\varepsilon}\big)-z^\varepsilon$. Note that for $v\in\mathrm{H}^1_0(\Omega)$ and by using (4.5), we find

$$\begin{aligned}&\int_{\Omega_f}\alpha_f\nabla\xi^\varepsilon\cdot\nabla v\,\mathrm{d}x+\int_{\Omega_m}\alpha_m\nabla\xi^\varepsilon\cdot\nabla v\,\mathrm{d}x+\int_{\Omega_f}(\alpha_f-\alpha_m)(\nabla u^0(0)-\nabla u^0)\cdot\nabla v\,\mathrm{d}x\\&=-\int_{\Omega_f}\alpha_f\nabla z^\varepsilon\cdot\nabla v\,\mathrm{d}x-\int_{\Omega_m}\alpha_m\nabla z^\varepsilon\cdot\nabla v\,\mathrm{d}x.\end{aligned}\tag{4.6}$$

Choosing $v=\xi^\varepsilon\in\mathrm{H}^1_0(\Omega)$ in (4.6), we get

$$\begin{aligned}&\alpha_f\left\|\nabla\xi^\varepsilon\right\|^2_{\mathrm{L}^2(\Omega_f)}+\alpha_m\left\|\nabla\xi^\varepsilon\right\|^2_{\mathrm{L}^2(\Omega_m)}+\int_{\Omega_f}(\alpha_f-\alpha_m)(\nabla u^0(0)-\nabla u^0)\cdot\nabla\xi^\varepsilon\,\mathrm{d}x\\&=\int_{\Omega_f}\alpha_f\nabla z^\varepsilon\cdot\nabla\xi^\varepsilon\,\mathrm{d}x+\int_{\Omega_m}\alpha_m\nabla z^\varepsilon\cdot\nabla\xi^\varepsilon\,\mathrm{d}x,\end{aligned}$$

which by using Cauchy-Schwarz's inequality leads to

$$\left\|\nabla\xi^\varepsilon\right\|_{\mathrm{L}^2(\Omega)}\le C\big(\left\|\nabla u^0(0)-\nabla u^0\right\|_{\mathrm{L}^2(\Omega_f)}+\left\|\nabla z^\varepsilon\right\|_{\mathrm{L}^2(\Omega)}\big).$$

According to Poincaré's inequality, we find

$$\left\|\xi^\varepsilon\right\|_{\mathrm{H}^1(\Omega)}\le C\big(\left\|\nabla u^0(0)-\nabla u^0\right\|_{\mathrm{L}^2(\Omega_f)}+\left\|z^\varepsilon\right\|_{\mathrm{H}^1(\Omega)}\big).$$

Notice that $\xi^\varepsilon=u-u^0-\varepsilon W^0\big(\frac{\cdot}{\varepsilon}\big)-z^\varepsilon$ allows to infer that

$$\left\|u-u^0-\varepsilon W^0\Big(\frac{\cdot}{\varepsilon}\Big)\right\|_{\mathrm{H}^1(\Omega)}\le C\big(\left\|\nabla u^0(0)-\nabla u^0\right\|_{\mathrm{L}^2(\Omega_f)}+\left\|z^\varepsilon\right\|_{\mathrm{H}^1(\Omega)}\big).\tag{4.7}$$

By using the continuity of the lifting operator from $\mathrm{H}^{1/2}(\Gamma)$ to $\mathrm{H}^1(\Omega)$, we get

$$\left\|u-u^0-\varepsilon W^0\Big(\frac{\cdot}{\varepsilon}\Big)\right\|_{\mathrm{H}^1(\Omega)}\le C\Big(\left\|\nabla u^0(0)-\nabla u^0\right\|_{\mathrm{L}^2(\Omega_f)}+\varepsilon\left\|W^0\Big(\frac{\cdot}{\varepsilon}\Big)\right\|_{\mathrm{H}^{1/2}(\Gamma)}\Big).\tag{4.8}$$

We evaluate now separately the two terms on the right hand side of (4.8). On the one hand, we observe that

$$\nabla u^0(x)=\nabla u^0(0)+\mathcal{O}(|x|).$$

Consequently, we find

$$\left\|\nabla u^0(x)-\nabla u^0(0)\right\|_{\mathrm{L}^2(\Omega_f)}\le C\left\|x\right\|_{\mathrm{L}^2(\Omega_f)}\le C\varepsilon^2.\tag{4.9}$$

On the other hand, the last term on the right hand side of (4.8) can be evaluated thanks to an expansion of W^0 in polar coordinates. Let $x \stackrel{\text{def}}{=} (r\cos(\theta), r\sin(\theta))$ for all $r \geq \varepsilon R_0$ with $R_0 > 1$. Since W^0 is an harmonic function, for all $n \in \mathbb{N}^*$ and $\theta \in [0, 2\pi]$, there exists $(\widetilde{a}_n, \widetilde{b}_n) \in \mathbb{R}^2$ such that

$$W^0\Big(\frac{x}{\varepsilon}\Big) = \sum_{n\geq 1}\Big(\frac{\varepsilon R_0}{r}\Big)^n (\widetilde{a}_n \cos(n\theta) + \widetilde{b}_n \sin(n\theta)). \tag{4.10}$$

Let Ω_c be a subset of $\mathbb{R}^2$ with $\Gamma \subset \mathring{\Omega}_c$, such that there exists $(\varrho_1, \varrho_2) \in \mathbb{R}^2$ with $\varrho_1 < |x| < \varrho_2$, for all $x \in \Omega_c$. Then, the trace inequality leads to

$$\Big\|W^0\Big(\frac{\cdot}{\varepsilon}\Big)\Big\|_{\mathrm{H}^{1/2}(\Gamma)} \leq C\|W^0\Big(\frac{\cdot}{\varepsilon}\Big)\Big\|_{\mathrm{H}^1(\Omega_c)}. \tag{4.11}$$

Choosing $\varepsilon > 0$ such that $\varepsilon < \frac{\varrho_1}{R_0}$, we get

$$\|W^0\Big(\frac{\cdot}{\varepsilon}\Big)\Big\|^2_{\mathrm{L}^2(\Omega_c)} \leq \frac{2\varepsilon^2 R_0^2 |\Omega_{\mathrm{c}}|}{\varrho_1^2} \sum_{k\geq 1}\Big(\frac{\varepsilon R_0}{\varrho_1}\Big)^{2(k-1)} \big(|\widetilde{a}_k|^2 + |\widetilde{b}_k|^2\big) \leq C\varepsilon^2, \tag{4.12a}$$

$$\Big\|\nabla W^0\Big(\frac{\cdot}{\varepsilon}\Big)\Big\|^2_{\mathrm{L}^2(\Omega_c)} \leq \frac{4\varepsilon^2 R_0^2 |\Omega_c|}{\varrho_1^2} \sum_{k\geq 1} k^2\Big(\frac{\varepsilon R_0}{\varrho_1}\Big)^{2(k-1)} \big(|\widetilde{a}_k|^2 + |\widetilde{b}_k|^2\big) \leq C\varepsilon^2, \tag{4.12b}$$

where $|\Omega_{\mathrm{c}}|$ stands for the usual measure of Ω_c. Introducing (4.12) into (4.11), we get

$$\Big\|W^0\Big(\frac{\cdot}{\varepsilon}\Big)\Big\|_{\mathrm{H}^{1/2}(\Gamma)} \leq C\varepsilon. \tag{4.13}$$

Carrying (4.9) and (4.13), we finally obtain (4.2). □

In order to make a comparison with respect to the size of the inclusion ε and the size of the patch, without changing its geometry, we introduce a fixed size patch $\widetilde{\Lambda} \subset \Omega$ (such that $\partial\widetilde{\Lambda} \cap \partial\Omega = \emptyset$). We consider $\Lambda = \frac{\widetilde{\Lambda}}{p}$ with $p > 1$. It is also convenient to introduce the following notation:

$$\begin{array}{rccc} h_p: & \widetilde{\Lambda} & \to & \Lambda \\ & u & \mapsto & u/p \end{array}$$

In the sequel, we denote by $\mathcal{L} : \mathrm{H}^{1/2}(\partial\widetilde{\Lambda}) \to \mathrm{H}^1(\widetilde{\Lambda})$ the continuous harmonic lifting operator in the fixed configuration. We define $\mathcal{L}_p : \mathcal{X} \to \mathrm{H}^1(\Lambda)$ as the scaled harmonic lifting operator, for all $f_p \in \mathcal{X}$ and $x \in \Lambda$, we get

$$(\mathcal{L}_p(f_p))(x) = (\mathcal{L}f)(px)$$

with $f(z) \stackrel{\text{def}}{=} f_p(z/p)$ for any $z \in \partial\widetilde{\Lambda}$. Notice that

$$\|\nabla(\mathcal{L}_p f_p)\|^2_{\mathrm{L}^2(\Lambda)} = \|\nabla(\mathcal{L}f)\|^2_{\mathrm{L}^2(\widetilde{\Lambda})}. \tag{4.14}$$

The following estimate between $W^0\big(\frac{\cdot}{\varepsilon}\big)$ and $\mathrm{Proj}_{\mathcal{W}_0}\big(W^0\big(\frac{\cdot}{\varepsilon}\big)\big)$ is an intermediate result which allow us to get an estimate between w^0 and $W^0\big(\frac{\cdot}{\varepsilon}\big)$.

Lemma 4.2. *There exists a constant $C > 0$, independent of ε and p, such that*

$$\left\| W^0\Big(\frac{\cdot}{\varepsilon}\Big) - \mathrm{Proj}_{\mathcal{W}_0}\Big(W^0\Big(\frac{\cdot}{\varepsilon}\Big)\Big)\right\|_{\alpha,\Lambda} \leq Cp\varepsilon. \tag{4.15}$$

Proof. Let $W_p \overset{\text{def}}{=} W^0\big(\frac{\cdot}{\varepsilon}\big) - \mathrm{Proj}_{\mathcal{W}_0}\big(W^0\big(\frac{\cdot}{\varepsilon}\big)\big)$, $W \overset{\text{def}}{=} W^0\big(\frac{\cdot}{p\varepsilon}\big)$, $f_p \overset{\text{def}}{=} W^0\big(\frac{\cdot}{\varepsilon}\big)_{|\partial\Lambda}$ and $f \overset{\text{def}}{=} W_{|\partial\widetilde{\Lambda}} = W^0\big(\frac{\cdot}{p\varepsilon}\big)_{|\partial\widetilde{\Lambda}}$. Observe that W_p is the unique solution of the following variational formulation:

$$\begin{cases} \text{find } W_p \in \mathrm{H}^1(\Lambda) \text{ with } W_p = f_p \text{ on } \partial\Lambda \text{ such that for all } z \in \mathcal{W}_0, \\ \displaystyle\int_\Lambda \alpha \nabla W_p \cdot \nabla z \,\mathrm{d}x = 0. \end{cases}$$

Hence, we can apply (3.18) to $\eta = W_p$ and $\zeta = \mathcal{L}_p f_p$, we find

$$\|W_p - \mathcal{L}_p f_p\|_{\alpha,\Lambda} \leq C_{\alpha_f,\alpha_m} \|\mathcal{L}_p f_p\|_{\alpha_f,\Omega_f} \leq C_{\alpha_f,\alpha_m} \|\mathcal{L}_p f_p\|_{\alpha,\Lambda}.$$

It follows that

$$\|W_p\|_{\alpha,\Lambda} \leq (1 + C_{\alpha_f,\alpha_m}) \max(\alpha_f,\alpha_m) \ \|\nabla(\mathcal{L}_p f_p)\|_{\mathrm{L}^2(\Lambda)} \leq (1 + C_{\alpha_f,\alpha_m}) \max(\alpha_f,\alpha_m) \ \|\nabla(\mathcal{L} f)\|_{\mathrm{L}^2(\widetilde{\Lambda})},$$

by (4.14). Finally, by using (4.13), we find

$$\|W_p\|_{\alpha,\Lambda} \leq C \max(\alpha_f,\alpha_m) \ \|f\|_{\mathrm{H}^{1/2}(\partial\widetilde{\Lambda})} \leq C \max(\alpha_f,\alpha_m) p\varepsilon.$$

□

We can now establish the following estimate between the corrector w^0 given by the patch method and $W^0\big(\frac{\cdot}{\varepsilon}\big)$ the corrector of the asymptotic analysis.

Lemma 4.3. *Let w^0 be the solution to Problem* (3.2) *for $n = 0$. Then, we have*

$$\left\| w^0 - \varepsilon W^0\Big(\frac{\cdot}{\varepsilon}\Big)\right\|_{\alpha,\Lambda} \leq Cp\varepsilon^2. \tag{4.16}$$

Proof. Note that the triangle inequality leads to

$$\left\| w^0 - \varepsilon W^0\Big(\frac{\cdot}{\varepsilon}\Big)\right\|_{\alpha,\Lambda} \leq \left\| w^0 - \mathrm{Proj}_{\mathcal{W}_0}\Big(\varepsilon W^0\Big(\frac{\cdot}{\varepsilon}\Big)\Big)\right\|_{\alpha,\Lambda} + \varepsilon \left\| \mathrm{Proj}_{\mathcal{W}_0}\Big(W^0\Big(\frac{\cdot}{\varepsilon}\Big)\Big) - W^0\Big(\frac{\cdot}{\varepsilon}\Big)\right\|_{\alpha,\Lambda}. \tag{4.17}$$

Since $w^0 = \mathrm{Proj}_{\mathcal{W}_0}(u - u^0)$, it comes that

$$\left\| w^0 - \mathrm{Proj}_{\mathcal{W}_0}\Big(\varepsilon W^0\Big(\frac{\cdot}{\varepsilon}\Big)\Big)\right\|_{\alpha,\Lambda} \leq \left\| \mathrm{Proj}_{\mathcal{W}_0}\Big(u - u^0 - \varepsilon W^0\Big(\frac{\cdot}{\varepsilon}\Big)\Big)\right\|_{\alpha,\Lambda} \leq \left\| u - u^0 - \varepsilon W^0\Big(\frac{\cdot}{\varepsilon}\Big)\right\|_{\alpha,\Lambda}. \tag{4.18}$$

According to inequality (4.17), Lemmas 4.1 and 4.2, (4.16) follows. □

On the one hand, we observe that

$$\|u - (u^0 + w^0)\|_{\alpha,\Lambda} \leq \|u - u^0 - \varepsilon W^0\Big(\frac{\cdot}{\varepsilon}\Big)\|_{\alpha,\Omega} + \left\| w^0 - \varepsilon W^0\Big(\frac{\cdot}{\varepsilon}\Big)\right\|_{\alpha,\Lambda} \leq C\varepsilon^2 + Cp\varepsilon^2 \leq Cp\varepsilon^2.$$

On the other hand, this implies

$$\begin{aligned}\|u-(u^0+w^0)\|_{\alpha,\Omega} &\leq \left\|u-u^0-\varepsilon W^0\Big(\frac{\cdot}{\varepsilon}\Big)\right\|_{\alpha,\Omega}+\left\|w^0-\varepsilon W^0\Big(\frac{\cdot}{\varepsilon}\Big)\right\|_{\alpha,\Omega}\\ &\leq \left\|u-u^0-\varepsilon W^0\Big(\frac{\cdot}{\varepsilon}\Big)\right\|_{\alpha,\Omega}+\left\|w^0-\varepsilon W^0\Big(\frac{\cdot}{\varepsilon}\Big)\right\|_{\alpha,\Lambda}+\varepsilon\left\|W^0\Big(\frac{\cdot}{\varepsilon}\Big)\right\|_{\alpha_m,\Omega\setminus\Lambda}\\ &\leq C\varepsilon^2+Cp\varepsilon^2+\varepsilon\left\|W^0\Big(\frac{\cdot}{\varepsilon}\Big)\right\|_{\alpha_m,\Omega\setminus\Lambda}.\end{aligned}$$

By using (4.12) for ϱ_1, which is the largest radius of the circle included in Λ, for $\varepsilon<\frac{\varrho_1}{R_0}$, we find

$$\left\|W^0\Big(\frac{\cdot}{\varepsilon}\Big)\right\|_{\alpha_m,\Omega\setminus\Lambda}\leq C\frac{\varepsilon}{\varrho_1}\leq Cp\varepsilon,$$

which implies that

$$\left\|u-(u^0+w^0)\right\|_{\alpha,\Omega}\leq Cp\varepsilon^2. \tag{4.19}$$

The next step consists to obtain an estimate for $\left\|\frac{\partial w^0}{\partial n}\right\|_{\mathcal{X}'}$.

Lemma 4.4. *There exists a constant $C>0$, independent of ε and p, such that*

$$\left\|\frac{\partial w^0}{\partial n}\right\|_{\mathcal{X}'}\leq Cp^{3/2}\varepsilon^2\leq\frac{C\varepsilon^2}{\mathrm{diam}(\Lambda)^{3/2}}. \tag{4.20}$$

Proof. We evaluate first $\|f\|_{\mathrm{H}^{1/2}(\partial\widetilde{\Lambda})}$ with respect to $\|f_p\|_{\mathcal{X}}$. To this aim, we define the linear operator $\mathcal{D}_p$ as follows

$$\begin{array}{rccc}\mathcal{D}_p: & \mathscr{H}(\partial\Lambda) & \to & \mathscr{H}(\partial\widetilde{\Lambda})\\ & f_p & \mapsto & f\end{array} \tag{4.21}$$

where $\mathscr{H}$ could be L^2, or $\mathrm{H}^{1/2}$ or H^1. On the one hand, we observe that

$$\|f\|^2_{\mathrm{L}^2(\partial\widetilde{\Lambda})}=\int_{\partial\widetilde{\Lambda}}|f(u)|^2\,\mathrm{d}S=\int_{\partial\widetilde{\Lambda}}|f_p(u/p)|^2\,\mathrm{d}S=p\,\|f_p\|^2_{\mathrm{L}^2(\partial\Lambda)},$$

and

$$\|\nabla f\|^2_{\mathrm{L}^2(\partial\widetilde{\Lambda})}=\int_{\partial\widetilde{\Lambda}}\frac{1}{p^2}|\nabla f_p(u/p)|^2\,\mathrm{d}S=\frac{1}{p}\,\|\nabla f_p\|^2_{\mathrm{L}^2(\partial\Lambda)}$$

for all $p\geq 1$. We deduce that

$$\begin{aligned}\|\mathcal{D}_p\|_{\mathrm{L}^2}&=\sup_{f_p\in\mathrm{L}^2(\partial\Lambda)}\frac{\|f\|_{\mathrm{L}^2(\partial\widetilde{\Lambda})}}{\|f_p\|_{\mathrm{L}^2(\partial\Lambda)}}=\sqrt{p},\\ \|\mathcal{D}_p\|_{\mathrm{H}^1}&=\sup_{f_p\in\mathrm{H}^1(\partial\Lambda)}\frac{\|f\|_{\mathrm{H}^1(\partial\widetilde{\Lambda})}}{\|f_p\|_{\mathrm{H}^1(\partial\Lambda)}}\leq\sqrt{p}+\frac{1}{\sqrt{p}}\ \text{with } p\geq 1.\end{aligned}$$

By interpolating [16], we find

$$\|\mathcal{D}_p\|_{\mathrm{H}^{1/2}}\leq C\,\|\mathcal{D}_p\|^{1/2}_{\mathrm{L}^2}\,\|\mathcal{D}_p\|^{1/2}_{\mathrm{H}^1}\leq C\sqrt{1+p},$$

with a constant $C > 0$ independent of $\varepsilon > 0$ and $p \geq 1$. Let $\theta \in \mathrm{C}^\infty(\widetilde{\Lambda}, [0,1])$ be a cut-off function which is such that $\theta(x) = 1$ for x in a small tubular neighborhood T of $\partial\widetilde{\Lambda}$ and $\theta(x) = 0$ outside a small tubular neighborhood containing T and $\theta_p = \theta \circ (h_p)^{-1}$. Using the regularity of w^0 and Green's formula, it comes that

$$\int_\Lambda \alpha \nabla w^0 \cdot \nabla(\theta_p \mathcal{L}_p f_p)\,\mathrm{d}x = \Big\langle \frac{\partial w^0}{\partial n}, f_p \Big\rangle_{\mathcal{X}',\mathcal{X}}$$

for all $f_p \in \mathrm{H}^{1/2}(\partial\Lambda)$. Denoting $\widetilde{\mathcal{T}} = \{x \in \widetilde{\Lambda} : \theta(x) > 0\}$ and $\mathcal{T} = \frac{\widetilde{\mathcal{T}}}{p}$, we deduce that

$$\Big|\Big\langle \frac{\partial w^0}{\partial n}, f_p \Big\rangle_{\mathcal{X}',\mathcal{X}}\Big| \leq \alpha_m \left\|\nabla w^0\right\|_{\mathrm{L}^2(\mathcal{T})} \left\|\nabla(\theta_p \mathcal{L}_p f_p)\right\|_{\mathrm{L}^2(\Lambda)} = \alpha_m \left\|\nabla w^0\right\|_{\mathrm{L}^2(\mathcal{T})} \left\|\nabla(\theta \mathcal{L} f)\right\|_{\mathrm{L}^2(\widetilde{\Lambda})}.$$

However, we have

$$\begin{aligned}\left\|\nabla(\theta\mathcal{L}f)\right\|_{\mathrm{L}^2(\widetilde{\Lambda})} &\leq \|\theta\|_{\mathrm{W}^{1,\infty}(\widetilde{\Lambda})} \|\mathcal{L}f\|_{\mathrm{H}^1(\widetilde{\Lambda})} \leq C \|f\|_{\mathrm{H}^{1/2}(\partial\widetilde{\Lambda})} \\ &\leq C \|\mathcal{D}_p f_p\|_{\mathrm{H}^{1/2}(\partial\widetilde{\Lambda})} \leq C \|\mathcal{D}_p\|_{\mathrm{H}^{1/2}} \ \|f_p\|_{\mathcal{X}} \leq C\sqrt{1+p}\,\|f_p\|_{\mathcal{X}},\end{aligned}$$

and

$$\left\|\nabla w^0\right\|_{\mathrm{L}^2(\mathcal{T})} \leq \left\|\nabla w^0 - \varepsilon \nabla W^0\Big(\frac{\cdot}{\varepsilon}\Big)\right\|_{\mathrm{L}^2(\Lambda)} + \varepsilon \left\|\nabla W^0\Big(\frac{\cdot}{\varepsilon}\Big)\right\|_{\mathrm{L}^2(\mathcal{T})}. \tag{4.22}$$

On the one hand, Lemma 4.3 leads to

$$\left\|\nabla w^0 - \varepsilon \nabla W^0\Big(\frac{\cdot}{\varepsilon}\Big)\right\|_{\mathrm{L}^2(\Lambda)} \leq Cp\varepsilon^2.$$

On the other hand, (4.12) and since $|x| > \varrho_1$ for $x \in \widetilde{\mathcal{T}}$, we get

$$\left\|\nabla W^0\Big(\frac{\cdot}{\varepsilon}\Big)\right\|_{\mathrm{L}^2(\mathcal{T})} = \left\|\nabla W^0\Big(\frac{\cdot}{p\varepsilon}\Big)\right\|_{\mathrm{L}^2(\widetilde{\mathcal{T}})} \leq Cp\varepsilon.$$

Consequently, we obtain

$$\Big|\Big\langle \frac{\partial w^0}{\partial n}, f_p \Big\rangle_{\mathcal{X}',\mathcal{X}}\Big| \leq Cp\varepsilon^2 \sqrt{1+p}\,\|f_p\|_{\mathcal{X}} \leq C\varepsilon^2 p^{3/2}\,\|f_p\|_{\mathcal{X}},$$

which proves the lemma. □

5 Numerical multi-scale patch method

We present in this section a multi-scale discrete patch method defined by the iterative patch procedure (3.1) and (3.2). To this aim, we introduce $\mathcal{T}^\Lambda$ and $\mathcal{T}^\Omega$ two non-degenerated, non-overlapping triangulations which are being respectively the polygonal domain partitions of Λ and Ω. More precisely, $\mathcal{T}^\Lambda$ is a refined mesh of Λ with maximal size equal to h and $\mathcal{T}^\Omega$ is a relatively coarse mesh of Ω with maximal size H. Furthermore, $\mathcal{T}^\Omega$ is taken conformal to the boundary of Λ for simplicity. In order to approximate u^n and w^n, we first introduce the following finite element spaces:

$$\mathcal{V}_0^H \stackrel{\text{def}}{=} \{v \in \mathrm{C}^0(\overline{\Omega}) : \text{ for all } K \text{ triangle of } \mathcal{T}^\Omega,\, v_{|K} \in P^k(K),\, v_{|_{\Gamma_\mathrm{D}}} = 0\} \subset \mathcal{V}_0,$$

$$\mathcal{W}_0^h \stackrel{\text{def}}{=} \{v \in \mathrm{C}^0(\overline{\Omega}) : \text{ for all } K \text{ triangle of } \mathcal{T}^\Lambda,\, v_{|K} \in P^k(K),\, v_{|_{\Omega\setminus\Lambda}} = 0\} \subset \mathcal{W}_0.$$

We assume also that the first terms of the discrete procedure satisfy $w_h^{-1} = u_H^{-1} = 0$. Hence for any w_h^{n-1} and u_H^{n-1} given, $n \geq 0$, we first solve the following macro problem on $\mathcal{T}^\Omega$:

$$\begin{cases} \text{find } u_H^n \in \mathcal{V}_0^H \text{ such that for all } v_H \in \mathcal{V}_0^H, \\ \displaystyle\int_\Omega \alpha_m \nabla u_H^n \cdot \nabla v_H \,\mathrm{d}x = \int_\Omega f v_H \,\mathrm{d}x + \int_{\Gamma_\mathrm{N}} h v_H \,\mathrm{dS} \\ \displaystyle -\int_{\Omega_f} (\alpha_f - \alpha_m) \nabla u_H^{n-1} \cdot \nabla v_H \,\mathrm{d}x - \int_\Lambda \alpha \nabla w_h^{n-1} \cdot \nabla v_H \,\mathrm{d}x, \end{cases} \tag{5.1}$$

and then we solve the following micro problem on $\mathcal{T}^\Lambda$:

$$\begin{cases} \text{find } w_h^n \in \mathcal{W}_0^h \text{ such that for all } v_h \in \mathcal{W}_0^h, \\ \displaystyle\int_\Lambda \alpha \nabla w_h^n \cdot \nabla v_h \,\mathrm{d}x = \int_\Lambda f v_h \,\mathrm{d}x - \int_\Lambda \alpha \nabla u_H^n \cdot \nabla v_h \,\mathrm{d}x. \end{cases} \tag{5.2}$$

From a numerical viewpoint, the micro and macro coupling terms in (5.1) and (5.2) are computed by using Gauss-quadrature formulas on the macro and micro meshes, respectively. Clearly, the solution w_h^{n-1} to the micro problem (5.2) (resp. u_H^n to the macro problem (5.1)) is implicitly employed in the macro problem (5.1) (resp. the micro problem (5.2)) through its orthogonal projection onto the space $\mathcal{V}_0^H$ (resp. $\mathcal{W}_0^h$) with respect to the scalar product $\langle \cdot, \cdot \rangle_{\alpha,\Lambda}$ (more rigorously by the scalar product induced by approximate integration). Let $u_{hH}^n \overset{\text{def}}{=} u_H^n + w_h^n$. The reader may notice that u_{hH}^n is an approximate solution of u (see (2.4)) on the nth iteration. We denote by $\mathcal{T}^{\text{ref}}$ a regular mesh with a maximal size h_{ref} be conformal to both boundaries $\partial\Lambda$ and Γ^ε. The reference solution u_{ref}, used later on in the numerical simulations, is the solution to the discrete variational formulation:

$$\begin{cases} \text{find } u \in \mathcal{V}_0^{h_{\text{ref}}} \text{ such that for all } v \in \mathcal{V}_0^{h_{\text{ref}}}, \\ \displaystyle\int_{\Omega_m} \alpha_m \nabla u \cdot \nabla v \,\mathrm{d}x + \int_{\Omega_f} \alpha_f \nabla u \cdot \nabla v \,\mathrm{d}x = \int_\Omega f v \,\mathrm{d}x + \int_{\Gamma_\mathrm{N}} h v \,\mathrm{dS}. \end{cases} \tag{5.3}$$

Assume that w_h^n and u_H^n converge to w_h and u_H, respectively, as n tends to ∞. It follows by adding (5.1) and (5.2) that

$$\int_\Omega \alpha \nabla (u_H + w_h) \cdot \nabla (v_H + v_h) \,\mathrm{d}x = \int_\Omega f (v_H + v_h) \,\mathrm{d}x + \int_{\Gamma_N} h (v_H + v_h) \,\mathrm{d}S,$$

for all $v_H \in \mathcal{V}_0^H$ and all $v_h \in \mathcal{W}_0^h$ which means that $u_{hH} = u_H + w_h$ is the best approximation to the solution on $\mathcal{V}_0^H + \mathcal{W}_0^h$.

6 Numerical examples

Let $\Omega = (-L, L) \times (-L, L)$ with $L = 10$. We assume that the boundary Γ is split into two distinct parts, namely, Dirichlet and Neumann boundaries denoted by $\Gamma_\mathrm{D} = (-L, L) \times \{-L\} \cup (-L, L) \times \{L\}$ and $\Gamma_\mathrm{N} = \{-L\} \times (-L, L) \cup \{L\} \times (-L, L)$, respectively, where homogeneous conditions are prescribed. Furthermore, we suppose that the inclusion is a disk of center $(3, 2)$ and radius ε (see Figure 2), while

the patch domain is a square $\Lambda = (3-l, 3+l) \times (2-l, 2+l)$. We choose the volumetric source term f equal to 10 $\cos(\frac{\pi}{4L}x)$ $\cosh(\frac{y}{2L})$. Note that the reference solution (see Figure 3(a)) is calculated on the reference mesh $\mathcal{T}^{\text{ref}}$ (see Figure 3(b)) while all the numerical simulations are performed by using a macro mesh $\mathcal{T}^{\Omega}$, which is conformal to the patch boundary $\partial\Lambda$.

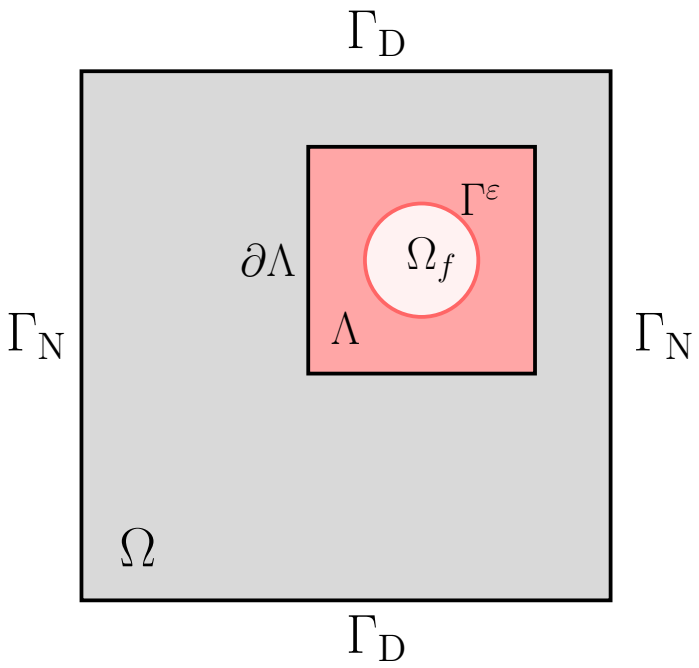

Figure 2: A simple square domain containing an inclusion and a patch.

6.1 Convergence of the iterations

6.1.1 Convergence of the iterations with a single mesh for the reference, micro and macro models

Our goal consists in this section to test the convergence of the iterations without the influence of the difference between the meshes (and the corresponding projections) of macro and micro problems by using the same mesh for the three problems, although this situation is not really of practical interest. When the convergence occurs and since $\mathcal{V}_0^H + \mathcal{W}_0^h = \mathcal{V}_0^H = \mathcal{V}_0^{h_{\text{ref}}}$, the iterations should converge toward the reference solution up to machine precision

We consider, in the numerical simulations, several values of the contrast between α_m and α_f and for $h = H = h_{\text{ref}} = \frac{L}{40}$. We illustrate the contrast impact between α_m and α_f on the solution by plotting the difference between the solutions associated to the reference model u_{ref} and the macro model (see Figures 4(a) and 4(b)). Recall that u_H^0 is the discrete solution of (2.2) without any inclusion.

The relative error rate in the $\text{H}^1(\Omega)$-norm between u_{ref} and u_{hH}^n is plotted in Figure 5 according to the variation of the iterations number n. We observe that the iterative procedure converges within few iterations. Since the convergence occurs for all tested contrast values, the results obtained by the numerical simulations are much better than expected by the theoretical results presented in Section 3.2.

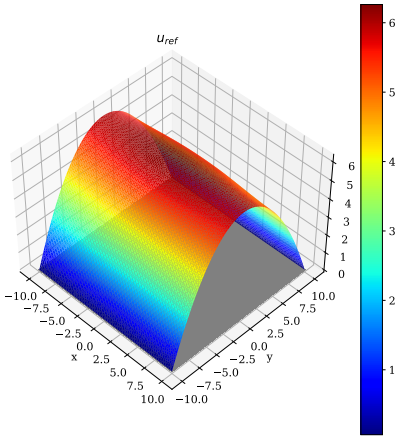

(a) Reference solution ($\alpha_m = 75$ and $\alpha_f = 100$)

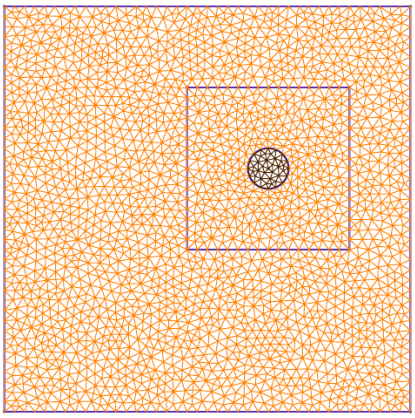

(b) Conformal mesh

Figure 3: A reference solution and an example of a conformal mesh with $h_{\text{ref}} = \frac{L}{20}$

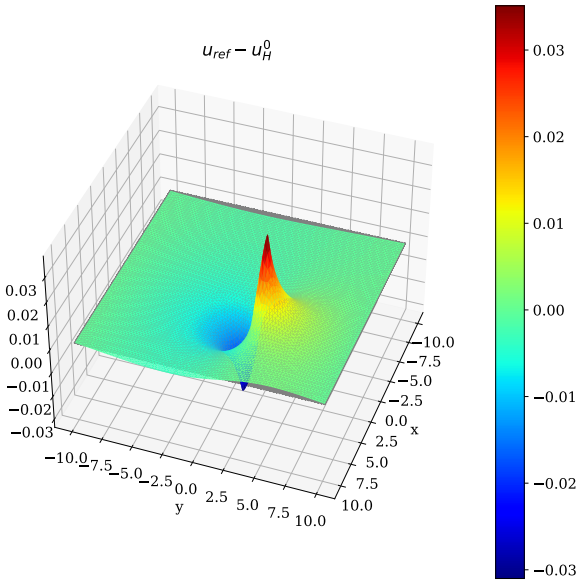

(a) $\alpha_m = 75$ and $\alpha_f = 100$

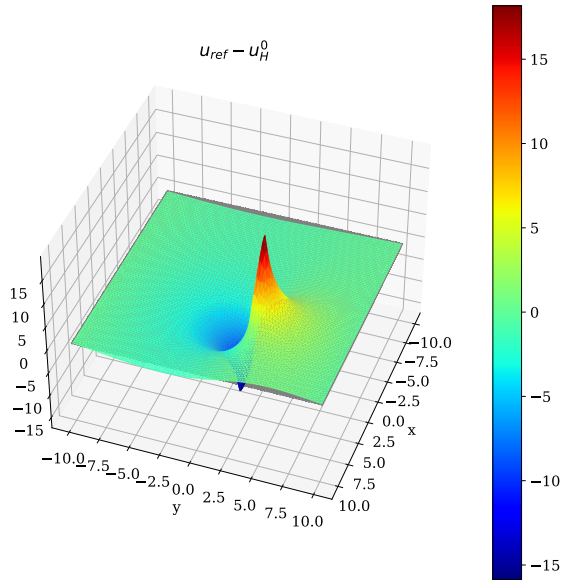

(b) $\alpha_m = 1$ and $\alpha_f = 100$

Figure 4: Plot of $u_{\text{ref}} - u_H^0$ for two different contrasts.

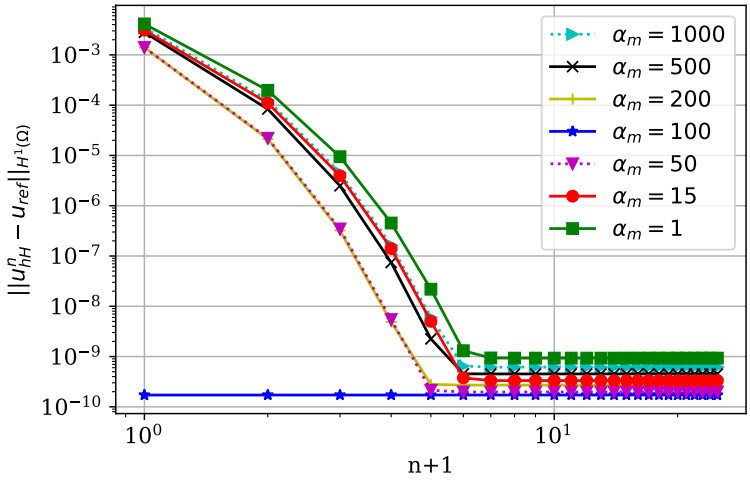

Figure 5: The relative error in $\mathrm{H}^1(\Omega)$-norm for different values of contrast (between α_m and $\alpha_f = 100$) and with the same mesh for the reference, micro and macro model ($h = H = h_{\mathrm{ref}} = \frac{L}{40}$).

6.1.2 Convergence of the iterations with non-matching meshes

In order to highlight the influence of the difference of meshes on micro and macro problems, we consider now three independent meshes. The reference solution is computed by using an adaptive mesh, where the maximum size near the inclusion is set as $h_{\mathrm{ref}} = \frac{L}{600}$, while in the remaining domain it is $\frac{L}{80}$. Furthermore, meshes are generated for the micro and macro models, having maximal sizes $h = \frac{L}{120}$ and $H = \frac{L}{40}$, respectively. Note that the mesh for the macro model is non-conformal to the inclusion boundary $\partial\Omega_f$.

We observe that if α_m satisfies $\alpha_m \geq 15$, the iterative procedure converges quickly for the $\mathrm{H}^1(\Omega)$-norm (see Figure 6). The relative error in the $\mathrm{H}^1(\Omega)$-norm is much more important compared to the case where the same mesh is used for the three models. While in the case where $\alpha_m < 15$, the error decreases during the first iterations, but the procedure finally diverges. Consequently, this scenario is less advantageous than the one involving identical meshes and aligns more closely with the theoretical outcomes presented in Section 3.2. which predict convergence for not too high contrast or for a sufficiently small inclusion. However, in both cases, the error resulting from halting after the second iteration is quite low.

Finally, we might note that the iterations convergence in the case where $\alpha_m < 15$ can be recovered by a refinement of the patch mesh (see Figure 7), i.e. by taking the micro mesh size h sufficiently small. Here we choose $H = \frac{L}{40}$, $\alpha_m = 1$ and $\alpha_f = 100$.

6.2 A relaxation method to recover the convergence

As an alternative approach to the refinement of the patch mesh, we propose below a relaxation method in the case of a high contrast.

Since Problem (5.2) corresponds to a descent method on the potential energy associated to the system in the direction w_h^n, it does not alter the iteration convergence. The non-convergence for high contrast

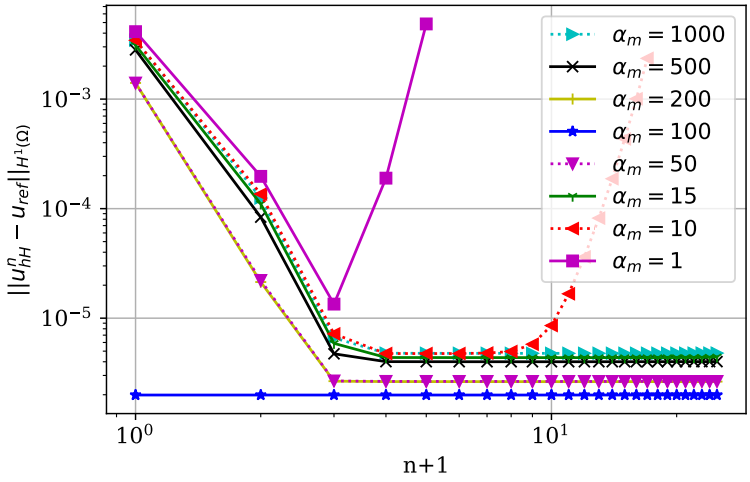

Figure 6: The relative error in $\mathrm{H}^1(\Omega)$-norm with respect to the variation of the number of iteration n for different values of contrast between α_m and $\alpha_f = 100$, non-matching meshes ($h = \frac{L}{120}, H = \frac{L}{40}$) and a non-conformal macro mesh with the inclusion $\partial\Omega_f$.

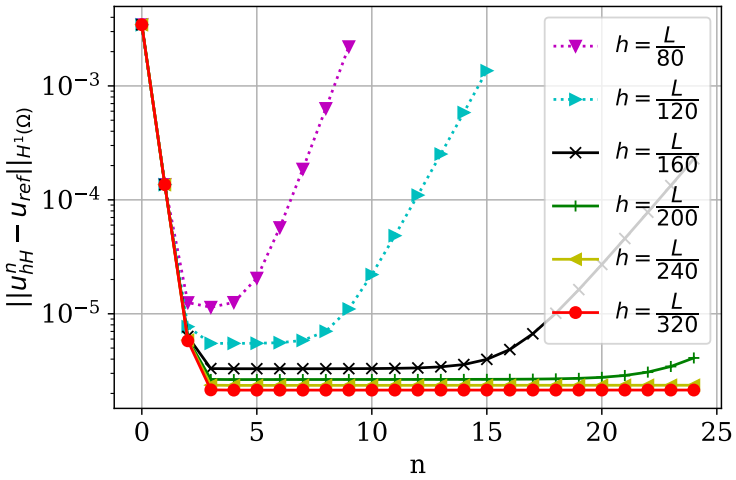

Figure 7: The relative error in $\mathrm{H}^1(\Omega)$-norm with respect to the variation of the number of iteration n for different values of micro-mesh size (with $\alpha_m = 10$ and $\alpha_f = 100$), non-matching meshes ($H = \frac{L}{40}$) and a non-conformal macro mesh with the inclusion $\partial\Omega_f$.

values arises from the term u_H^{n-1} in (5.1). This term follows the asymptotic expansion and ensures that u_H^0 is the solution without the inclusion. Furthermore, w_h^0 is close to the first corrector of the asymptotic

expansion and globally u_H^n is a smooth solution which does not take into account the local variations across the interface between the matrix and the inclusion which is handled by w_h^n. To lower the influence of this term on the convergence, we propose to introduce a relaxation keeping u_H^0 and w_h^0 unchanged and, for $\beta \in (0,1)$ a relaxation coefficient, to modify from the second iteration as follows:

- denoting now $\widetilde{u}_H^n$ a solution to (5.1) for $n \geq 1$ and taking $u_H^n = \beta \widetilde{u}_H^n + (1-\beta) u_H^{n-1}$ instead $\widetilde{u}_H^n$.
- the remaining is unchanged, in particular, w_h^n is still a solution to (5.2).

Note that this relaxation method is applied only to the step (5.1) and, thus, it slightly differs from the relaxation method proposed in [21]. Looking at Figure 8, it is clear that with a sufficiently low relaxation coefficient (specifically, $\beta \leq 0.05$ in this scenario), our iterative approach can recover convergence even under high-contrast conditions (with $\alpha_m = 1$ and $\alpha_f = 100$). However, the cost of this restored convergence is an elevation in the requisite number of iterations for achieving convergence.

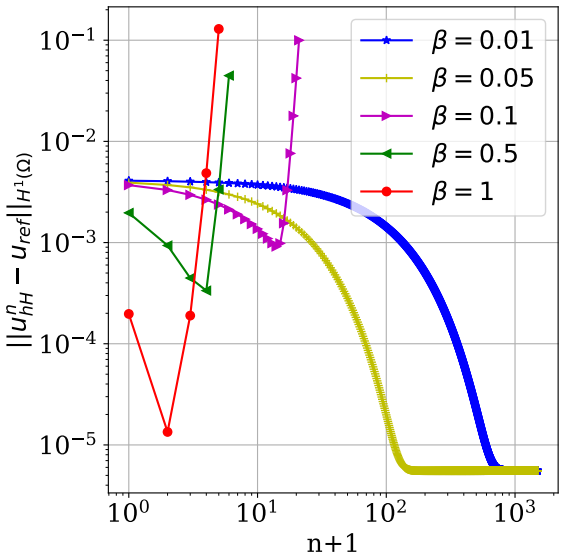

Figure 8: The relative error in $\mathrm{H}^1(\Omega)$-norm with respect to the variation of the number of iteration n for different values of the relaxation coefficient (with $\alpha_m = 1$ and $\alpha_f = 100$), non-matching meshes ($h = \frac{L}{120}$, $H = \frac{L}{40}$) and a non-conformal macro mesh with the inclusion $\partial\Omega_f$.

6.3 Influence of the size of the patch

In this section the reference solution is calculated by using an adaptive mesh with a maximal size h_{ref} equal to $\frac{L}{600}$ in the inclusion vicinity and $\frac{L}{80}$ in the remained domain. In order to study the effect of the patch domain size on the accuracy of the obtained solution by the multi-scale patch strategy, we plot in Figure 9 the relative error in $\mathrm{L}^2(\Omega)$ and $\mathrm{H}^1(\Omega)$ norms according to the patch characteristic parameter p with $h = \frac{L}{80}$, $H = \frac{L}{40}$ and a non-conformal mesh with the boundary $\partial\Omega_f$ for the macro model. As

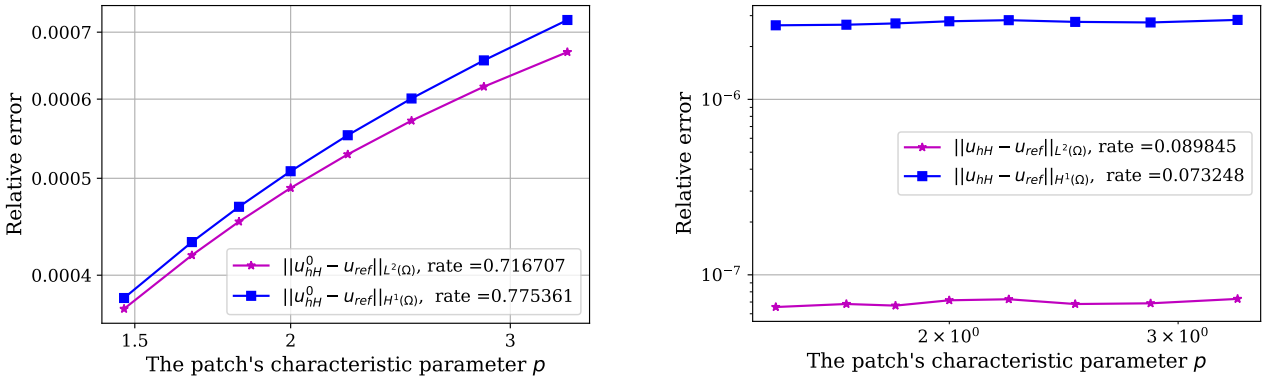

(a) First iteration

(b) Last iteration

Figure 9: The relative error in $\mathrm{L}^2(\Omega)$ and $\mathrm{H}^1(\Omega)$ norms for the first and last iteration of the iterative method with respect to the patch characteristic parameter p with $h = \frac{L}{80}$, $H = \frac{L}{40}$ and a non-conformal mesh with the macro model boundary $\partial\Omega_f$.

expected, we observe that the relative error between u^0_{hH} and u_{ref}, decreases in both $\mathrm{L}^2(\Omega)$ and $\mathrm{H}^1(\Omega)$ norms, when the patch size increase (see the Figure 9(a)). Note that the convergence rate of order 1 in $\mathrm{H}^1(\Omega)$-norm given by the theoretical estimate (4.19) is not fully reached for large value of p. This corresponds to patch sizes close to the inclusion size for which there is probably some side effects. On the other hand, the relative errors between u_{hH} and u_{ref}, in both $\mathrm{L}^2(\Omega)$ and $\mathrm{H}^1(\Omega)$ norms, remain almost constant when the patch size varies (see the Figure 9(b)). Consequently, we conclude that the choice of a relatively small patch can be compensated by using an adequate iterations number of the proposed method.

6.4 Influence of the inclusion size

In this section, the reference mesh (resp. the micro mesh) is conformal to circles with radius $\epsilon_1 = 1.5, \epsilon_2 = 1, \epsilon_3 = 0.5$, and $\epsilon_4 = 0.25$. The maximum size of the reference mesh (resp. the micro mesh) near each circle $i\,(1 \leq i \leq 4)$ is $h_{\text{ref}} = \epsilon_i/40$ (resp. $h = \epsilon_i/20$), while in the remaining domain, it is equal to $L/80$ (resp. $L/40$). The macro mesh is non-conformal to the inclusion boundary $\partial\Omega_f$ and possesses a maximum size H equal to $L/40$. In order to study the effect of the inclusion size on the solution accuracy, we first plot in Figure 10 the variation of the relative error in $\mathrm{L}^2(\Omega)$ and $\mathrm{H}^1(\Omega)$ norms according to the size of the inclusion. We observe that the relative error between u^0_{hH} and u_{ref}, in both $\mathrm{L}^2(\Omega)$ and $\mathrm{H}^1(\Omega)$ norms, decreases when the size of the inclusion decreases (see Figure 10(a)). The convergence rate are approximately of order 2 for both $\mathrm{L}^2(\Omega)$ and $\mathrm{H}^1(\Omega)$ relative error norms. Such a convergence rate confirms the result in (4.19). Furthermore, the Figure 10(b) shows that the relative error between u_{hH} and u_{ref}, in both $\mathrm{L}^2(\Omega)$ and $\mathrm{H}^1(\Omega)$ norms, also decreases being several order of magnitude smaller than for the first iteration. However, a certain saturation of the error can be observed, probably due to the difference in element sizes between the reference mesh and the macro and micro meshes. We plot on the Figure 11 the

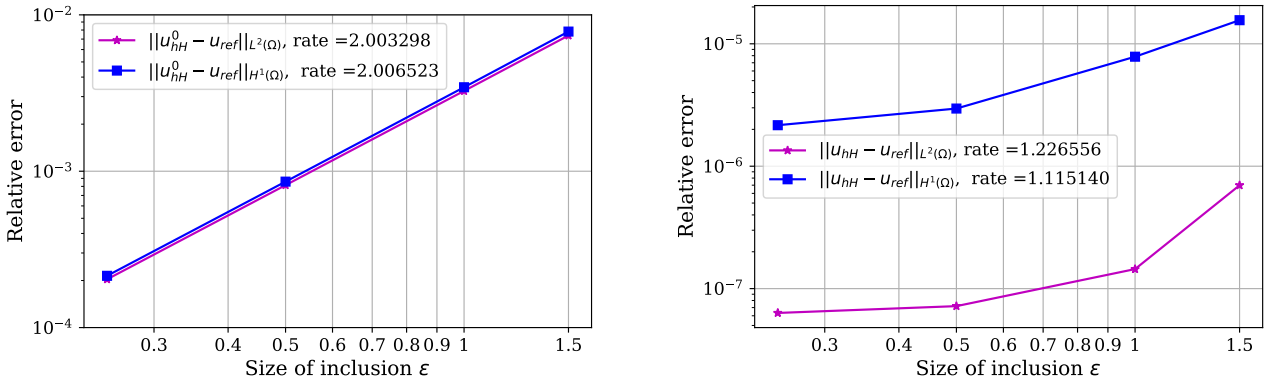

(a) First iteration

(b) Last iteration

Figure 10: The relative error in $\mathrm{L}^2(\Omega)$ and $\mathrm{H}^1(\Omega)$ norms according to the size of the inclusion ε with a non-conformal mesh with the macro model boundary $\partial\Omega_f$.

relative error in $\mathrm{H}^1(\Omega)$ norm according to the number of iterations n for three values of ε with $\alpha_m = 5$, $\alpha_f = 100$, $h_{\text{ref}} = \frac{L}{2000}$, $h = \frac{\varepsilon}{20}$, $H = \frac{L}{40}$ and a non-conformal mesh with the boundary $\partial\Omega_f$ for the macro model. We observe that the iterative method diverges when $\varepsilon = 1$ but it converges for a smaller value of ϵ, specifically $\varepsilon \leq 0.5$, confirming the outcome stated in the Proposition 3.4.

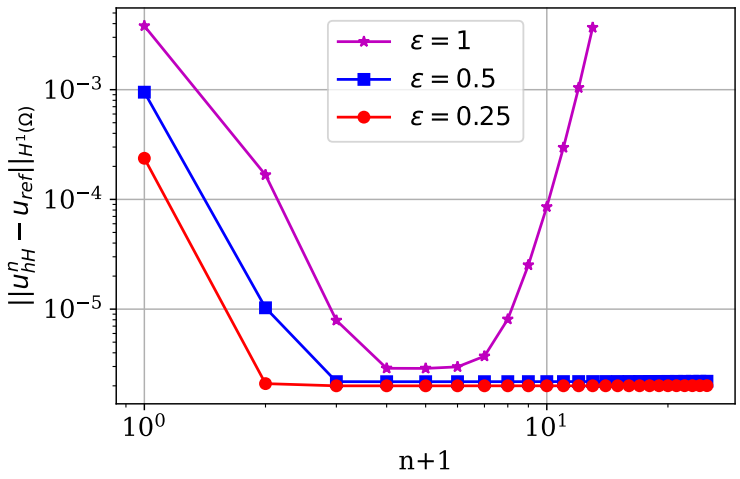

Figure 11: Evolution through iterations of the relative error in $\mathrm{H}^1(\Omega)$-norms for three inclusion sizes.

Conclusion

We presented in this work an iterative patch method for a problem with a small inhomogeneity. The main interest of this method is that it starts from the problem without inclusion, which allows to use a standard code to compute the large scale solution without meshing the inclusion. The method build a local corrector on a patch surrounding the inclusion leading to a robust solution as long as the inclusion is small enough (or the contrast between the coefficient is small enough) and the patch is sufficiently large. Furthermore, an iterative procedure allows to converge to the best finite element approximation, at least for a small inclusion or contrast as well.

We obtained some theoretical results for the iterations convergence of our patch method and we established some convergence order with respect to the inclusion and patch sizes. These results, together with the presented numerical examples, indicate that the first iteration corrector allows to improve the solution in all the cases. This means that is many cases, no supplementary iteration is necessary to get an accurate approximation.

The numerical examples highlight that the numerical multi-scale patching method convergence is not ensured for high value of the contrast of stiffnesses in accordance with our theoretical results. For an unclear reason, this limitation is not noted in the numerical results when the meshes for the micro and macro problems are the same (which of course does not really correspond to a situation in agreement with the objectives of the proposed method), and also when the mesh for the micro problem is sufficiently refined. We proposed then a relaxation method to recover the convergence for arbitrary meshes.

Some natural perspectives for further work are extensions to the nonlinear case of finite deformation problems and to the case of multiple inclusions.

Acknowledgments

We would like to especially thank the company "Manufacture Française des Pneumatiques Michelin" for the financial and technical support.

References

[1] G. Allaire. *Shape optimization by the homogenization method.* Volume 146 of Applied Mathematical Sciences, Springer-Verlag, New York (2002).

[2] H. Ammari, H. Kang. *Reconstruction of small inhomogeneities from boundary measurements.* Springer-Verlag, Berlin Heidelberg (2004).

[3] C. Amrouche, V. Girault, J. Giroire. Weighted Sobolev spaces for Laplace's equation in $\mathbb{R}^n$. *J. Math. Pures Appl.*, 73, (1994), 579-606.

[4] Y. Antipov, P. Schiavone. On the uniformity of stresses inside an inhomogeneity of arbitrary shape *Int. J. Eng. Sci.*, 68, (2003), 299-311.

[5] M. Arfaoui, M. R. Ben Hassine, M. Moakher, Y. Renard, G. Vial. Multi-scale asymptotic expansion for a small inclusion in elastic media. *Journal of Elasticity*, 131, (2018), 207-237.

[6] A. Bendali, K. Lemrabet. The effect of a thin coating on the scattering of a time-harmonic wave for the Helmholtz equation. *SIAM J. Appl. Math.*, 56(6), (1996), 1664-1693.

[7] E. Beretta, E. Bonnetier, E. Francini, A. L. Mazzucato. An asymptotic formula for the displacement field in the presence of small anisotropic elastic inclusions. *Inverse Problems and Imaging*, 6, (2012), 1-23.

[8] E. Bonnetier, F. Triki. Asymptotics in the presence of inclusions of small volume for a conduction equation: A case with a non-smooth reference potential. *Contemp. Math.*, 494, (2009), 95-107.

[9] H. Brezis. *Progress in Nonlinear Differential Equations and Their Applications: In memory of Pierre Grisvard* Birkhäuser, Boston (1996).

[10] A. Chagneau. *Méthode de zoom structural étendue aux hétérogénéités non linéaires.* PhD thesis, University of Montpellier (2019).

[11] M. Dambrine, G. Vial. Influence of a boundary perforation on a Dirichlet energy *Control and Cybernetics*, 34(1), (2005), 117-136.

[12] M. Dambrine, G. Vial. A multi-scale correction method for local singular perturbations of the boundary. *Math. Model. Numer. Anal.*, 41(1), (2007), 111-127.

[13] L. Daridon, D. Dureisseix, S. Garcia, S. Pagano. Changement d'échelles et zoom structural. Proceeding of the 10th CSMA Colloquium, (2011).

[14] P. Dolean, P. Jolivet, F. Nataf. *An introduction to domain decomposition methods: algorithms, theory, and parallel implementation.* SIAM, 2015.

[15] A. Ern, J.-L. Guermond. *Theory and Practice of Finite Elements.* Springer-Verlag, New York (2004).

[16] J. Bergh, J. Löfström. *Interpolation spaces: an introduction.* Springer Science & Business Media (2012).

[17] J. D. Eshelby. The determination of the elastic field of an ellipsoidal inclusion, and related problems. *Proceedings of the Royal Society of London. Series A, Mathematical and Physical Sciences*, 241, (1957), 376-396.

[18] J. D. Eshelby. The elastic field outside an ellipsoidal inclusion. *Proceedings of the Royal Society of London. Series A, Mathematical and Physical Sciences*, 252, (1959), 561-569.

[19] A. Fortin, A. Garon. *Les Éléments Finis de la Théorie à la Pratique.* Université Laval Ecole Polytechnique de Montréal, Montréal (2011).

[20] G. Geymonat, F. Krasucki, S. Lenci. Mathematical analysis of a bonded joint with a soft thin adhesive. *Math. Mech. Solids*, 4(2), (1999), 201-225.

[21] R. Glowinski, J. He, A. Lozinski, J. Rappaz, J. Wagner. Finite element approximation of multi-scale elliptic problems using patches of elements. *Numerische Mathematik*, 101, (2005), 663-687.

[22] D. J. Hansen, C. Poignard, M. S. Vogelius. Asymptotically precise norm estimates of scattering from a small circular inhomogeneity. *Appl. Anal.*, 86(4), (2007), 433-458.

[23] A. Heibig, N. Mannai, A. Petrov, Y. Renard. A thick-point approximation of a small body embedded in an elastic medium: justification with an asymptotic analysis. *ZAMM Z. Angew. Math. Mech.*, 101 (2021), no. 10, 19 pp.

[24] E. Kröner. Statistical Modelling. In J. Gittus and J. Zarka, editors, Modelling Small Deformations of Polycrystals, Springer, Dordrecht, the Netherlands (1986), 229-291.

[25] E. Kröner. Modified Green Functions in the Theory of Heterogeneous and/or Anisotropic Linearly Elastic Media. In G. J. Weng, M. Taya, and H. Ab, editors Micromechanics and Inhomogeneity: The Toshio Mura 65th Anniversary Volume, Springer, New York, NY (1990), 197-211.

[26] D. Leguillon, E. Sánchez-Palencia. *Computation of singular solutions in elliptic problems and elasticity.* Masson, Paris (2002).

[27] S. Li, R. Sauer, G. Wang. A circular inclusion in a finite domain I. The Dirichlet-Eshelby problem. *Acta Mechanica*, 179(1), (2005), 67-90.

[28] E. Lignon. *Modélisation multi-échelles de nappes fibrés en compression.* Ph.D. thesis, Ecole Polytechnique (2011).

[29] J.–L. Lions, E. Magenes. *Problèmes aux limites non homogènes et applications.* Vol. 1. (French) Travaux et Recherches Mathématiques N°17 Dunod, Paris (1968).

[30] A. Lozinski, J. Rappaz, J. Wagner. Finite Element Method with Patches for Poisson problems in polygonal domains. *In ESAIM: Proceedings, 21, (2007), pp. 45-64.*

[31] P. Mazilu. On the theory of linear elasticity in statically homogeneous media. *Rev. Roum. Math. Pur. Appl.*, 17, (1972), 261–273.

[32] V. Rezzonico, A. Lozinski, M. Picasso, J. Rappaz, J. Wagner. Multiscale algorithm with patches of finite elements. *Mathematics and Computers in Simulation, 76(2007), pp. 181-187.*

[33] W. Rudin. *Real and complex analysis.* Second edition. McGraw-Hill Series in Higher Mathematics. McGraw-Hill Book Co., New York-Düsseldorf-Johannesburg, 1974. xii+452 pp.

[34] E. Sánchez–Palencia. Problèmes de perturbations liés aux phénomènes de conduction à travers des couches minces de grande résistivité. *J. Math. Pures Appl.*, 53(9), (1974), 251–269.

[35] P. Schiavone. Neutrality of the elliptic inhomogeneity in the case of non-uniform loading. *IMA journal of applied mathematics*, 8, (2003), 161–169.

[36] G. Vial. *Analyse multi–échelle et conditions aux limites approchées pour un problème avec couche mince dans un domaine à coins.* PhD thesis Université de Rennes 1 (2003).